

See discussions, stats, and author profiles for this publication at: <https://www.researchgate.net/publication/26833955>

Theory of passive additive-pulse mode locking

Article *in* Optics Letters · July 1991

DOI: 10.1364/OL.16.001104 · Source: PubMed

CITATIONS

4

READS

8

1 author:



Jyhyng Wang

152 PUBLICATIONS 1,521 CITATIONS

SEE PROFILE

Theory of passive additive-pulse mode locking

Jyhpyng Wang

*Institute of Atomic and Molecular Sciences, Academia Sinica, and
Department of Electrical Engineering, National Taiwan University, Taipei, Taiwan*

Received February 7, 1991

The laser configuration of newly developed additive-pulse mode locking, also known as coupled-cavity mode locking, can be viewed as an intracavity interferometer. By solving the equation of motion of the two coupled cavities, a mathematical description of the self-starting mechanism is obtained. With this method, the transient pulse evolution of an initial seed pulse can be calculated and thereby optimized. The structure of the equation of motion suggests new single-cavity configurations of additive-pulse mode locking, and the same method of analysis can be applied to them.

In the past few years a new mode-locking method has been developed. This method employs feedback from a nonlinear coupled cavity to shorten the laser pulses. It was first demonstrated in the soliton laser^{1,2} and then achieved in many solid-state lasers.³⁻⁷ Now it is generally referred to as additive-pulse, or coupled-cavity, mode locking. With this method, pulse shortening by 2 orders of magnitude is commonly achieved. Recently it was further shown that, in a $\text{Ti:Al}_2\text{O}_3$ laser, frequency-tunable femtosecond pulses can be generated with this method without first actively mode locking the laser.⁸ The operation is all passive and self-starting. Since then self-starting mode locking has also been demonstrated in many other solid-state lasers.⁹⁻¹³

An additive-pulse mode-locking laser can be viewed as an intracavity interferometer with a nonlinear phase modulator. A short piece of optical fiber is utilized as the phase modulator. Self-phase modulation in the fiber produces a phase difference between the peak and the wings of the pulse. This phase modulation is translated into an amplitude modulation at the beam splitter (the output coupler of the main cavity). When the lengths of the two cavities are properly set, this amplitude modulation favors the growth of the peak and thereby mode locks the laser.

In this Letter the laser system shown schematically in Fig. 1(B), which is also the system in Ref. 8, is analyzed. It is assumed that the coupled-cavity laser is already pulsed. Initial pulses may come from mode beating or noise.¹⁴ Since the initial pulses or noise are much longer than the optical cycle, one can write the electric field as $E(t - z/c) \exp[i\omega(t - z/c)]$, where $E(t - z/c)$ is a slowly varying function and z and t are the spatial and time coordinates, respectively, or simply as $E(\tau) \exp(i\omega\tau)$, where τ is the reduced time, measuring the distance from the pulse center. To solve the equation of motion, the electric field is separated into two parts, $A(\tau) \exp(i\omega\tau)$, the field in the main laser cavity, and $B(\tau) \exp(i\omega\tau)$, the field in the external coupled cavity, propagating toward the beam splitter (output coupler

of the main cavity). $A(\tau)$ and $B(\tau)$ are both slowly varying and carry the phase of the fields. The two fields $A(\tau)$ and $B(\tau)$ add at the beam splitter once each round trip. Since in the starting stage the pulse is evolving, $A(\tau)$ and $B(\tau)$ are different on each round trip. Therefore we may label them $A_n(\tau)$ and $B_n(\tau)$, according to the number of round trips, n . The equation of motion of two empty coupled cavities with matched cavity lengths is

$$\begin{bmatrix} A_{n+1}(\tau) \\ B_{n+1}(\tau) \end{bmatrix} = \begin{bmatrix} R & iT \\ iT & R \end{bmatrix} \begin{bmatrix} A_n(\tau) \\ B_n(\tau) \end{bmatrix}, \quad (1)$$

where R is the square root of the power reflectivity of the beam splitter and T is the square root of the power transmission. If now the gain is added to the main cavity, and the loss to the external cavity, and a slight cavity length mismatch is introduced, then the equation of motion becomes [see Fig. 1(A)]

$$\begin{bmatrix} A_{n+1}(\tau) \\ B_{n+1}(\tau) \end{bmatrix} = \begin{bmatrix} Rg & iTg \\ iTle^{i\phi} & Rle^{i\phi} \end{bmatrix} \begin{bmatrix} A_n(\tau) \\ B_n(\tau) \end{bmatrix}, \quad (2)$$

where g is the square root of power gain, $1 - l^2$ is the power loss, and ϕ is the phase difference due to the slight cavity length mismatch. Equation (2) can be solved with a standard eigenvalue method. Let λ_1 and λ_2 be the two eigenvalues of the transformation matrix in Eq. (2); then the solution of Eq. (2) can be written as

$$\begin{bmatrix} C_{n+1}(\tau) \\ D_{n+1}(\tau) \end{bmatrix} = \begin{bmatrix} \lambda_1 & \\ & \lambda_2 \end{bmatrix} \begin{bmatrix} C_n(\tau) \\ D_n(\tau) \end{bmatrix},$$

$$\lambda = \frac{R(g + le^{i\phi}) \pm [R^2(g + le^{i\phi})^2 - 4gl e^{i\phi}]^{1/2}}{2}, \quad (3)$$

or, equivalently,

$$C_n(\tau) = \lambda_1^n C_0(\tau), \quad D_n(\tau) = \lambda_2^n D_0(\tau), \quad (4)$$

where $C_n(\tau)$ and $D_n(\tau)$ are linear combinations of $A_n(\tau)$ and $B_n(\tau)$ and can be thought of as the two eigenmodes of the coupled cavities. It can be shown easily on a computer that, for practical values of R , l , and g , there are regions of ϕ where the absolute value of one of the λ 's is larger than one, while the other

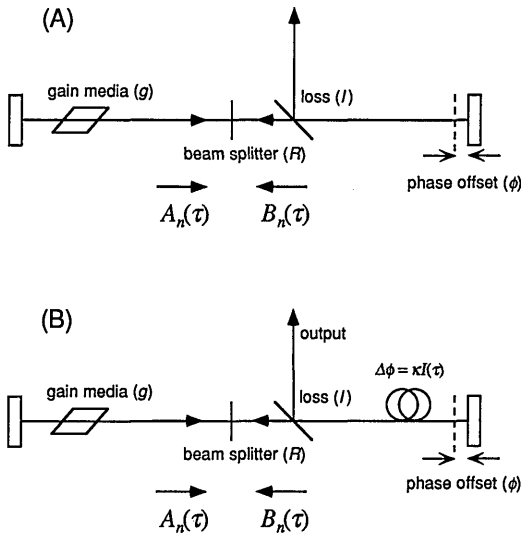


Fig. 1. (A) Schematic diagram of an intracavity interferometer, with gain in one arm and loss in the other. (B) An intracavity interferometer with a nonlinear phase modulator, to which an additive-pulse mode-locking laser is equivalent.

is smaller than one. Therefore in these regions one of the eigenmodes, say $D_n(\tau)$, is damped, while the other will grow with time. Although $|\lambda_1|$, the gain of $C_n(\tau)$, is larger than one initially, it will drop to one in the steady state because of gain saturation in the laser media. In other words, as the energy of the pulse grows higher and higher, g will drop according to

$$g = \exp\left(\frac{g_0 L}{1 + \frac{I_a}{I_s}} - \alpha L\right) \quad (5)$$

until $|\lambda_1| = 1$. In Eq. (5), g_0 is the small-signal exponential gain, I_a is the average intensity in the gain media, and I_s is the saturation intensity. The term αL represents the absorption of the gain media at lasing wavelength, with α the absorption coefficient and L the thickness of the gain media. When g is adjusted to make $|\lambda_1| = 1$, the numerical fact that $|\lambda_2|$ is smaller than one does not change.

In Eq. (5) it is assumed that the gain cross section is small, so that the gain saturates slowly compared with the pulse duration and the round-trip time. Therefore g has no dependence on τ . This is a good approximation for most of the solid-state lasers because of their small emission cross sections. A theoretical consideration of the effect of dynamic gain saturation on self-starting additive-pulse mode locking can be found in Ref. 15.

Now a phase modulation that is a function of τ is introduced. In the case of self-phase modulation [Fig. 1(B)], the phase difference ϕ becomes $\phi_0 + \kappa I(\tau)$, where ϕ_0 is the phase difference due to slight cavity length difference and $\kappa I(\tau)$ is due to the self-phase modulation and proportional to the instantaneous intensity $I(\tau)$. The parameter κ is positive and proportional to the fiber length and the nonlinear index of refraction, n_2 , of the fiber. Since the round-trip gain λ_1 depends on τ through ϕ , different portions of the pulse have different amplitude gain.

This differential gain for different parts of the pulse is the origin of pulse formation and shortening. If one can find an operating point so that in the neighborhood of that point $|\lambda_1|$ increases with ϕ , then the gain of the pulse peak will be higher than the pulse wings, because the phase of the peak is larger. In this case the energy in the pulse will gradually shift to the peak and thereby shorten the pulse. The mode-locking force f can be defined by

$$f \equiv \frac{\partial |\lambda_1|}{\partial \phi}, \quad (6)$$

evaluated at the operating point. If an operating point with $f > 0$ can be found, then pulse shortening can happen. It should be noted that the gain g is fixed by the saturation condition; it is not a free parameter of f . The mode-locking force f depends only on three parameters, the loss factor l , the coupling factor R , and the phase difference ϕ .

The mode-locking force of the Ti:Al₂O₃ laser in Ref. 8 has been calculated. The result is shown in Fig. 2, where the mode-locking force and the amplitude gain g are plotted against the phase difference ϕ_0 of the two cavities. Between zero and π the mode-locking force is positive, and it peaks near zero. While it is between $-\pi$ and zero, the mode-locking force is negative. In this region the laser favors a cw instead of a pulsing mode. In the neighborhood of zero phase, no data are shown, because in that region the value of g required exceeds the upper limit set by the small-signal gain $\exp(g_0 L - \alpha L)$. Intuitively, one would think that the mode-locking force would peak exactly at zero, because an interferometer described by Eq. (1) is most sensitive to phase variations at this phase difference. However, this is true only when one assumes that the two pulses leaving the beam splitter have the same phase. Such an assumption is not true in general.

The pulse-shortening rate is directly related to the differential gain Δg , defined by $\Delta g \equiv |\lambda_1|_{\text{peak}} - |\lambda_1|_{\text{wing}}$. Δg is proportional to the mode-locking force f , the average intensity in the fiber I_f , and inversely proportional to the pulse duration τ_p ,

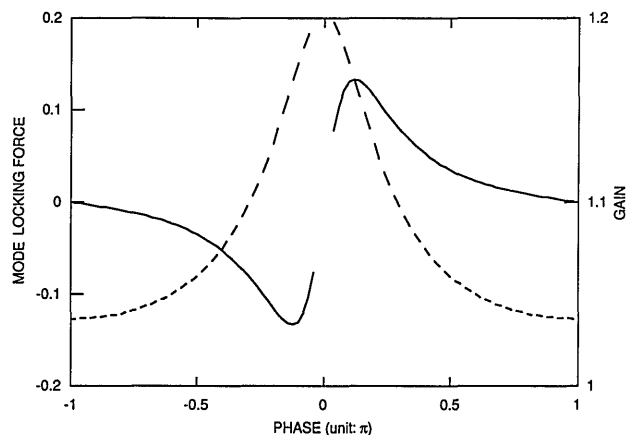


Fig. 2. Solid curve, the mode-locking force $\partial |\lambda_1| / \partial \phi$ as a function of the phase difference. Dashed curve, the round-trip amplitude gain of the laser. [The parameters are (from Ref. 8) $R = 0.92$ and $l = 0.387$.]

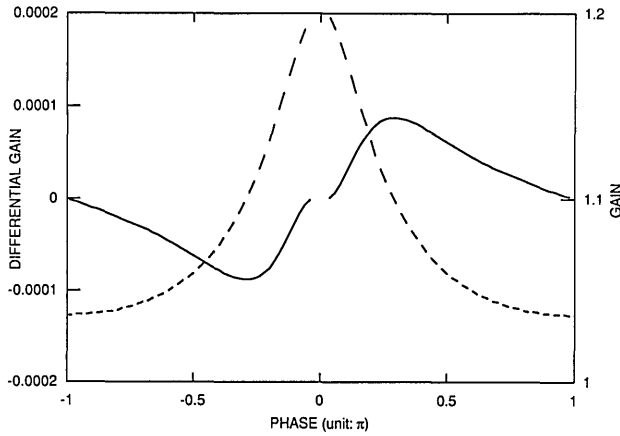


Fig. 3. Solid curve, the initial self-starting differential gain as a function of the phase difference. Dashed curve, the round-trip amplitude gain of the laser. [The parameters are (from Ref. 8) $\kappa = 0.00384/W$, $I_f \approx 200$ mW, $\tau_p = 6$ ns, $t_r = 12$ ns, $g_0 L = 0.36$, and $\alpha L = 0.185$.]

$$\begin{aligned} \Delta g &= \frac{\partial |\lambda_1|}{\partial I} (I_{\text{peak}} - I_{\text{wing}}) \\ &= \frac{\partial |\lambda_1|}{\partial \phi} \frac{d\phi}{dI} (I_{\text{peak}} - I_{\text{wing}}) = f \kappa \frac{I_f t_r}{\tau_p}, \end{aligned} \quad (7)$$

where t_r is the cavity round-trip time and I_{peak} and I_{wing} are the instantaneous intensities of the laser radiation in the fiber at the pulse peak and wings. To optimize the pulse-shortening rate, one should maximize Δg . Although Δg cannot be expressed in an analytical form, general optimization can be carried out with graphical methods on a computer. To calculate Δg , the first step is to determine g from the condition $|\lambda_1| = 1$, then calculate the average intensity in the gain media from Eq. (5). I_f is proportional to the intensity in the gain media and can be calculated from the setup of the laser. From I_f and Eq. (7), Δg can be obtained.

In Fig. 3 the differential gain Δg as well as the gain of the laser g are plotted as a function of the phase difference ϕ . It is seen that the region where Δg is significantly larger than zero occupies less than half of the 2π range. According to this theory, mode locking can happen only in this region. Such a conclusion is consistent with the experimental result in Ref. 16. The slope of g in this region is nonzero, which explains why the laser can be stabilized with a feedback circuit monitoring the cw average intensity.⁸ The time that it takes for the pulse to shorten to a steady state can be estimated from Δg to be 20,000 to 30,000 round trips. This also agrees with the experimental result in Ref. 17. Compared with that in Fig. 2, the maximum peak in Fig. 3 is shifted toward the right, because the average intensity of the laser increases with increasing phase in that region, as indicated by the falling curve of g .

In this Letter the effects of gain bandwidth and group-velocity dispersion are not included. This is

because in the self-starting stage, the initial pulse width is on the scale of the cavity round-trip time, which is long enough that these effects are not important. In the steady state, however, the pulse width, shape, and stability are related crucially to the bandwidth and dispersion factors. An analysis of the steady-state pulse can be found in Ref. 16.

The analysis presented in this Letter is general enough to suggest other possible forms of additive-pulse mode locking. For example, if the two arms of Fig. 1 are folded into a single ring cavity, the two counterpropagating modes, one clockwise and one counterclockwise, will interfere with each other at the beam splitter. The equation of motion has the same structure as the coupled-cavity case. The constant phase offset between the two modes can be provided by a Faraday rotator and $\lambda/4$ wave plates. Similarly, one could also imagine a single linear cavity, with two modes of perpendicular polarizations. An off-axis wave plate serves as the coupler between the two modes; an on-axis wave plate produces a constant phase offset between them. Because of the similarity in the equation of motion, these new possibilities can also be analyzed with the same method.

We thank J. Goodberlet, E. P. Ippen, H. A. Haus, and J. G. Fujimoto of the Massachusetts Institute of Technology for helpful discussions.

References

1. L. F. Mollenauer and R. H. Stolen, *Opt. Lett.* **9**, 13 (1984).
2. F. M. Mitschke and L. F. Mollenauer, *IEEE J. Quantum Electron.* **QE-22**, 2242 (1986).
3. K. J. Blow and D. P. Nelson, *Opt. Lett.* **13**, 1026 (1988).
4. P. N. Kean, X. Zhu, D. W. Crust, R. S. Grant, N. Langford, and W. Sibbett, *Opt. Lett.* **14**, 39 (1989).
5. J. Mark, L. Y. Liu, K. L. Hall, H. A. Haus, and E. P. Ippen, *Opt. Lett.* **14**, 48 (1989).
6. C. P. Yakymyshyn, J. F. Pinto, and C. R. Pollock, *Opt. Lett.* **14**, 621 (1989).
7. P. M. W. French, J. A. R. Williams, and J. R. Taylor, *Opt. Lett.* **14**, 686 (1989).
8. J. Goodberlet, J. Wang, J. G. Fujimoto, and P. A. Schulz, *Opt. Lett.* **14**, 1125 (1989).
9. J. Goodberlet, J. Jacobson, J. G. Fujimoto, P. A. Schulz, and T. Y. Fan, *Opt. Lett.* **15**, 504 (1990).
10. L. Y. Liu, J. M. Huxley, E. P. Ippen, and H. A. Haus, *Opt. Lett.* **15**, 553 (1990).
11. J. M. Liu and J. K. Chee, *Opt. Lett.* **15**, 685 (1990).
12. F. Krausz, Ch. Spielmann, T. Brabec, E. Wintner, and A. J. Schmidt, *Opt. Lett.* **15**, 737, 1082 (1990).
13. G. P. A. Malcolm, P. F. Curley, and A. I. Ferguson, *Opt. Lett.* **15**, 1303 (1990).
14. F. Krausz, T. Brabec, and Ch. Spielmann, *Opt. Lett.* **16**, 235 (1991).
15. E. P. Ippen, L. Y. Liu, and H. A. Haus, *Opt. Lett.* **15**, 183 (1990).
16. E. P. Ippen, H. A. Haus, and L. Y. Liu, *J. Opt. Soc. Am. B* **6**, 1736 (1989).
17. J. Goodberlet, J. Wang, J. G. Fujimoto, and P. A. Schulz, *Opt. Lett.* **15**, 1300 (1990).